Two-decade satellite monitoring of surface phytoplankton functional types in the Atlantic Ocean

Hongyan Xi[1*], Marine Bretagnon[2], Svetlana N. Losa[1,3], Vanda Brotas[4], Mara Gomes[4], Ilka Peeken[1], Antoine Mangin[2], Astrid Bracher[1,5]

[1]Alfred Wegener Institute, Helmholtz-Centre for Polar and Marine Research, Bremerhaven, 27570, Germany
[2]ACRI-ST, Sophia Antipolis Cedex, France
[3] Shirshov Institute of Oceanology, Russian Academy of Sciences, Moscow, Russia
[4]MARE/ARNET - Marine and Environmental Sciences Centre, Faculdade de Ciências, Universidade de Lisboa, Campo Grande, 1749-016, Lisboa, Portugal
[5]Institute of Environmental Physics, University of Bremen, Bremen, 28359, Germany

Correspondence to: Hongyan Xi (hongyan.xi@awi.de)

Abstract. An analysis of multi-satellite derived products of four major phytoplankton functional types (PFTs – diatoms, haptophytes, prokaryotes and dinoflagellates), was carried out to investigate the PFT time series in the trans-Atlantic Ocean between 2002 and 2021. The investigation includes the two-decade trends, climatology, phenology and anomaly of PFTs for the whole Atlantic Ocean and its different biogeochemical provinces in the surface layer that optical satellite signals can reach. The PFT time series over the whole Atlantic region showed mostly no clear trend over the last two decades, except for a small decline in prokaryotes and an abrupt increase in diatoms during 2018-2019 which is mainly observed in northern Longhurst provinces. The phenology of diatoms, haptophytes and dinoflagellates are very similar: in the higher latitudes bloom maxima are reached in spring (April in the northern and October in the southern hemisphere), in the oligotrophic regions in winter time, and in the tropical regions during May to September. Prokaryotes show in general opposite annual cycles to the other three PFTs and present more spatial complexity. The PFT anomaly (in percentage) of 2021 compared to the 20-year mean reveals mostly a slight decrease in diatoms and a prominent increase in haptophytes in most areas of the high latitudes. Both diatoms and prokaryotes show a mild decrease along coastlines and an increase in the gyres, while prokaryotes show a clear decrease in the mid- to low latitudes and an increase in the western African coast (CNRY and GUIN) and southwest corner of NATR. Dinoflagellates, as a minor contributor to the total biomass, are relatively stable in the whole Atlantic region. This study illustrated the past and current PFT state in the Atlantic Ocean, and acted as the first step to promote long-term consistent PFT observations that enable time series analyses of PFT trends and inter-annual variability, to reveal potential climate induced changes in phytoplankton composition on multiple temporal and spatial scales.

Short Summary. Continuous monitoring of phytoplankton groups using satellite data is crucial for understanding global ocean phytoplankton variability on different scales both in space and time. This study focuses on four important phytoplankton groups in the Atlantic Ocean to investigate their trend, anomaly and phenological characteristics over both the whole region

and subscales. This study paves the way to promote potentially important ocean monitoring indicators to help sustain the ocean health.

1 Introduction

Phytoplankton in the sunlit layer of the ocean act as the base of the marine food web fuelling fisheries, and also regulate key biogeochemical processes. Climate induced changes causing temperature rise, ocean acidification and ocean deoxygenation, stress the ocean's contemporary biogeochemical cycles and ecosystems, thereby impact the phytoplankton communities (Gruber, 2011; 2021; Bindoff et al. 2019). Related to this, the changing nutrient and light availability, particular in the polar oceans, are also critical for the development of phytoplankton communities (Käse and Geuer, 2018). In the past decades, satellite observations of ocean colour (OC) information, especially the surface chlorophyll a concentration (Chla) as a proxy of phytoplankton biomass, have been able to revolutionize our understanding of biogeochemical processes and provide insights of the changes in phytoplankton and inferred productivity driven by climate change (e.g., Antoine et al., 2005; Gregg and Rousseaux, 2014; McClain, 2009; Behrenfeld et al., 2016; Kulk et al., 2020). However, phytoplankton biomass does not provide a full description of the complex nature of phytoplankton community and function. Phytoplankton composition varies across ocean biomes and the different phytoplankton groups influence marine ecosystem and biogeochemical processes differently (Bracher et al., 2017). Continuous monitoring of phytoplankton composition is important not only to understand the biogeochemical processes such as nutrient uptake, carbon and energy transfer, but also for fisheries, ocean environment, water quality and even human health when certain species cause, for example, harmful algal blooms (Le Quéré et al., 2005; Bindoff et al. 2019; Bracher et al., 2022).

Phytoplankton diversity is very high, summarised in phytoplankton functional types (PFT) as prokaryotes (cyanobacteria) and eukaryotes, including diatoms, haptophytes, dinoflagellates. Depending on area, season, and size class, different PFT can act as dominating organisms in the food web and, therefore, regulate the seasonality of the predators (Käse and Geuer, 2018). Diatoms, known as major silicifiers have silica frustules that surround and protect the cells and sink rapidly out of the surface layer of the ocean contributing to the transport of carbon, nitrogen and silica to deeper waters (IOCCG, 2014). Haptophytes are another very abundant PFT in the global ocean occurring mainly in the middle-sized (2-20 μm) range. The prominent subgroup within haptophytes are coccolithophores, which have been considered a critical component of marine environments because of its dual capacity to fix environmental carbon via biomineralization (calcium carbonate, calcite) and through photosynthesis (Reyes-Prieto et al. 2009). Dinoflagellates are also one of the largest groups of marine eukaryotes, although most species are, in average, smaller than the average of diatom species. The majority of dinoflagellate species is autotrophic and tend to thrive under stable conditions. Due to their motility and ability of regulating their position in the water column, they can out-compete other phytoplankton, and sometime accumulate rapidly resulting in a visible coloration of the water, known as harmful algal blooms (IOCCG, 2014). Prokaryotes as picophytoplankton are abundant in many ocean regions

(notably in the mid to low latitudes but also others) and also account for a substantial fraction of marine primary production, with the two taxa being *Synechococcus* and *Prochlorococcus* in tropical regions (Flombaum et al., 2013).

PFTs have been the focus of various studies carried out worldwide as well as in the Atlantic Ocean, providing rich and valuable knowledge of PFT assessments in terms of their abundance, distribution, phenology, roles in the primary production and relations to other physical and biological parameters (e.g., Head and Pepin, 2010; Brotas et al., 2013, 2022; Soppa et al., 2016; Brewin et al., 2017; Moisan et al., 2017; Bolaños et al., 2020; Yang et al., 2020). Information of phytoplankton composition with respect to the functional types and size classes can be retrieved by ocean colour algorithms based on different types of input data. However, most of the studies focus on either a certain PFT (e.g., Lange et al., 2020), a short time period or a limited spatial coverage (e.g., Bracher et al., 2020; Brotas et al., 2022). A complete, systematic frame for the long-term monitoring of multiple PFTs on a wide scale is yet to be established. Previously, we have developed and further improved a set of empirical-orthogonal-function based PFT algorithms (referred to as EOF-PFT) thanks to a large global in-situ PFT data set based on HPLC (High Performance Liquid Chromatography) measured pigments (Xi et al., 2020; 2021). These algorithms use multi-spectral reflectance data from OC satellites and sea surface temperature data to estimate Chla concentration of six major phytoplankton groups. Here, we focus only on four PFTs, which on the whole account for the major part of the biomass in the Atlantic Ocean. Applied to multi-sensor merged products and Sentinel-3 OLCI data, the algorithms enable us to generate global PFT products which have been available on the EU Copernicus Marine Service since 2020 and updated timely, providing global chlorophyll *a* data with per-pixel uncertainty for diatoms, haptophytes, dinoflagellates, chlorophytes and phototrophic prokaryotes spanning the period from 2002 until today.

In this section, we combine these PFT data sets of different sensors, covering various lifespans and radiometric characteristics into long term consistent satellite PFT products. The two-decades quality-assured global PFT data sets for the Atlantic Ocean (50°S to 50°N, 60°W to 10°E) are derived by correcting the input sensor specific PFT products using inter-sensor comparisons with uncertainty estimations, which then allow us to 1) evaluate Copernicus Marine Service PFT products and improve their continuity along the products derived from different satellite sensors and 2) analyze PFT time series in the last two decades in terms of climatology, trends, anomaly and phenology of multiple PFTs in the Atlantic Ocean and its different biogeochemical provinces (Longhurst, 2007).

2 Data and method

2.1 PFT products from Copernicus Marine Service

Satellite data used in this study are listed in Table 1. Multiple PFT Chla products with per-pixel uncertainty have been available on Copernicus Marine Service since May 2020 with updates in 2021 and 2022, which were derived from three sets of OC products: 1) merged remote sensing reflectance (Rrs) products at 9 bands from SeaWiFS, MODIS and MERIS from July 2002 to December 2011, 2) merged Rrs products at 9 bands from MODIS and VIIRS from January 2012 to December 2016, and 3)

Rrs products at 11 bands from Sentinel 3A OLCI from January 2017 to December 2021 (Table 1, Xi et al., 2021). In this section, monthly PFT products with 25-km resolution in the open ocean (depth > 200 m) are used for spatiotemporal analysis in the Atlantic Ocean spanning the period from July 2002 to December 2021.

Consistency of satellite data is checked with the following details. As the product developer we have additionally generated PFT retrievals from different sensor combinations but with overlapping time periods. PFT products from SeaWiFS/MODIS/MERIS merged data and that from MODIS/VIIRS merged data have a 4-month overlap from January to April 2012, and MODIS/VIIRS derived PFTs are overlapped with the OLCI derived PFTs since May 2016. To produce consistent PFT products over the last two decades for the Atlantic Ocean, we compare PFT retrievals within these overlapped periods to identify the systematic differences between two data sources and then set up the correction functions through linear regressions by taking into account the per-pixel uncertainty. Sections 2.3 and 3.3 in Xi et al (2021) may be referred to for a detailed description of the per-pixel uncertainty assessment of the PFT products. Similar to how the OC-CCI Chl-a product was merged (OC-CCI v5.0 User Guide), one from the three sets of PFT products, that has been verified to have the lowest uncertainties (produced on pixel basis) and smallest biases when evaluated by in situ, will be chosen as the reference product. The other two sets of PFT products will be corrected to it. In the EOF-PFT approach development stage (Xi et al. 2020, 2021), we have noticed that the PFT products derived from SeaWiFS/MODIS/MERIS merged Rrs data have shown lowest per-pixel uncertainties nearly for all the PFT quantities, because their corresponding algorithms were trained based on a larger and more widely covered matchup data set between the satellite and in situ. Therefore, we take SeaWiFS/MODIS/MERIS derived PFTs as reference to correct the other two PFT data sets derived from MODIS/VIIRS merged and OLCI data, respectively.

2.2 In situ PFT data and matchup extraction

To evaluate the satellite PFT products, we use in situ HPLC pigment data from past expeditions between 2009 and 2019 covering the whole Atlantic polar to polar region (65°S to 80°N) which included ten expeditions from the North Atlantic to the Arctic Fram Strait (PS74, PSS76, PS78, PS80, PS85, PS93, PS99, PS106, PS107, PS121) and four expeditions in the trans-Atlantic Ocean (PS113, PS120, AMT28 and AMT29). All pigment data were quality controlled by applying the method by Aiken et al. (2009). Diagnostic pigment analysis was carried out to determine the in situ PFT Chla concentrations, following Xi et al. (2021) according to Vidussi et al. (2001) and Uitz et al. (2006) modified as in Hirata et al. (2011) and Brewin et al. (2015). In situ PFT data are then used to validate the corrected PFTs by extracting matchups between daily 4-km PFT products on Copernicus Marine Service and the in situ data. For each in situ measurement a matchup of 3×3 pixels around the in situ location on the same day was extracted. Averaged data based on 3×3 pixels were computed following the matchup protocol as in Xi et al. (2020, 2021), including only matchups containing at least 50% of valid pixels with a coefficient of variation (CV) of the valid pixel values lower than 0.15.

2.3 Time series analysis

We focus on preliminary explorations of the calibrated PFT products to reveal and understand the trends and variations of Atlantic PFTs in the last two decades. We derive the PFT time series on the whole Atlantic region, different regional scales and also per-pixel level. For regional scales, PFT data of the Atlantic Ocean are partitioned into smaller regions using Longhurst's geographic classification system of biomes and provinces (Longhurst, 2007; Flanders Marine Institute, 2009). We determine the annual cycle (climatology) based on both pixel data and regional log-based mean values, and derive anomalies to observe the inter-annual changes and detect trends reflected by the satellite observations. Time series analysis is done both per-pixel and for the whole region or province. We investigate the trends in the PFTs for the last 20 years using linear regression in the format of Y=SX+I, where Y is the monthly PFT Chla of either per-pixel or the regional log-based mean, X is the time on monthly basis, S is the slope of the regression and I is the intercept. Only trends with statistically significant correlations of the regression ($p<0.05$) are shown. Indicators of PFT phenology and the anomaly of 2021 (the last year of the considered time period) are also extracted in order to identify potential changes/shifts in PFTs. Abundance maxima time, as one of the phenology indicators, is identified for each pixel by finding the month when the maximum PFT Chla occurred during the year. Anomaly in percentage is determined by computing the relative difference between the PFT state of 2021 and the average state of the last two decades (i.e., climatology).

3 Results

3.1 Inter-sensor corrections of PFT products and validation with in situ data

Figure 1 shows the comparison between monthly PFTs from SeaWiFS/MODIS/MERIS merged and MODIS/VIIRS merged data for the overlapped four months (January – April 2012). PFT retrievals from different satellite sensors show some differences but overall correlate well with each other (R^2 >0.82). Type II linear regression between the retrievals from two satellite data sources is determined for each PFT by accounting for the per-pixel uncertainty. The slope and intercept values are then used to correct the MODIS/VIIRS derived PFTs to the SeaWiFS/MODIS/MERIS derived ones so that they are overall consistent though the pixelwise discrepancy still exists. The same is applied to the Sentinel 3A OLCI derived PFTs by comparing them to the corrected MODIS/VIIRS derived PFTs for the overlapped period April – December 2016, so that all PFT data from both MODIS/VIIRS and OLCI are now referenced to SeaWiFS/MODIS/MERIS derived PFTs. Though R^2 is slightly weaker (R^2 between 0.77 and 0.83) compared to that from the MODIS/VIIRS versus SeaWiFS/MODIS/MERIS derived PFTs (R^2 between 0.82 and 0.98), OLCI derived PFTs still showed overall good correlations to the corrected MODIS/VIIRS data with regression slopes between 0.83 and 1.03 despite that prokaryote Chla retrievals from OLCI data are in general higher.

Validation was carried out by comparing the collocated satellite PFTs with the in situ PFTs using the extracted matchup data. Statistical results of the validation in Table 2 show in general acceptable agreement between the in situ and satellite derived

PFTs. Median percent differences (MDPD) are consistent with the median satellite PFT uncertainties (relative error in %) estimated through Monte Carlo simulation and error propagation in Xi et al. (2021), and for dinoflagellates, notably lower. Higher MDPD is found for prokaryotes due to a systematic overestimation of the picophytoplankton in the retrieval algorithms for all the three sets of satellite OC sensors, however, no significant bias of satellite prokaryote products is detected between different sensors, therefore the overestimation should have minor influence on the time series data of prokaryotes. In addition, a coarser evaluation by directly comparing the monthly satellite PFT (which have better spatial coverage) to the in situ PFT for the whole cruise track, has shown that the PFT variation regarding regional phytoplankton dynamics observed by the in situ PFT is very well revealed by satellite PFT maps (images not shown). These evaluations assure the quality of the satellite PFTs for time series analysis.

3.2 PFT climatology (2002-2021)

Figure 2 shows the climatology (2002–2021) of the four PFTs generated using satellite monthly PFT products, depicting differences and similarities in terms of PFT Chla magnitude and spatial variation among different PFTs. Diatoms, as major silicifiers are typically large-celled (>20 μm, though species with smaller cells also exist) and highly dependent on nutrient levels. They are sensitive to the global temperature especially to the equator-pole temperature gradient. Two-decade climatology of diatoms in the Atlantic region shows clearly higher abundance in high latitudes and coastal regions and lowest abundance (or even undetectable) in the vast subtropical gyres. Similarly, haptophytes which are mostly classified as nanophytoplankton (2-20 μm), have also higher abundance in high latitudes and coastal regions, but span a larger coverage than diatoms. Enhanced abundance level is also found in the equatorial belt. Lowest abundance of haptophytes also locates in the gyres, but are not as low as diatoms. Prokaryotes, commonly referred to as picophytoplankton (<2 μm), show the highest abundance in the mid-low latitudes of the open Atlantic Ocean. Though spatially showing the lowest abundance in the gyres, prokaryotes are still the most dominant phytoplankton group in the majority of these regions. Dinoflagellates as a relatively minor contributor to the total biomass follow the similar distribution pattern of diatoms, but are much lower in abundance in higher latitudes.

3.3 PFT trends during 2002-2021 in the Atlantic Ocean

PFT annual cycle over the whole Atlantic Ocean: Following the climatology study, the annual cycles of the four PFTs are also derived by extracting the mean biomass of the two decades for each month (Fig. 3a). Prokaryotes are clearly the most dominant group showing the highest mean of the Chla (0.062 – 0.072 mg m^{-3}) over the Atlantic all year round, followed by haptophyte Chla which varies from 0.03 to 0.045 mg m^{-3}. Diatom Chla varies from 0.017 to 0.026 mg m^{-3} and dinoflagellates with the lowest mean Chla below 0.015 mg m^{-3}. Despite different magnitudes, diatoms, haptophytes and dinoflagellates present very similar annual cycles with two biomass peaks in April and November, indicating the spring blooming especially in the high

latitudes in both north and south hemispheres. In contrast, prokaryotes show a distinct biomass peak in June-July and a less prominent increase in December-January due to the suppressed growth of the other PFTs in these periods.

Time series of the monthly PFT data averaged for the whole Atlantic are shown in Fig. 3b, depicting a significant decrease (0.0001 Chla mg m^{-3} $month^{-1}$, $p<0.01$) in prokaryote Chla, but no significant trend is observed for the other three PFTs although some interannual changes are visible. Between the time window of 2003 and 2008, a slight decline in prokaryote Chla is observed followed by a two-year increase (2009-2010), but from 2011 onwards a continuous decline is again observed. Per-pixel trend of prokaryotes in Fig. 3e shows that the decreasing trend of prokaryotes is mainly found in the low latitudes and particularly in the west coast of Africa (provinces CNRY and GUIN, refer to Fig. 4 for Longhurst provinces). Haptophytes time series show lowest abundance during 2013 – 2015 which is then elevated slightly since 2016 (Fig. 3b). Slight increasing trend of haptophytes on the pixel level is found in the mid- to low latitude and a decrease is found near the coast in higher latitudes (Fig. 3d). Diatom Chla is rather stable until 2017 until an abrupt increase in 2018 – 2019, and then decreases in 2020 – 2021 to the average level of the last 20 years (Fig. 3b). Per-pixel time series in Fig. 3c shows that significant decrease is found only in the west coast of Africa (CNRY), northwest of the North Atlantic (NWCS), and Patagonian coast. A very slight increasing trend of diatoms is presented in the gyres and equatorial region. Dinoflagellate Chla contributes a very minor proportion to the total biomass (<10%) and are relatively stable in the last two decades in the whole Atlantic region (Figs. 3b and 3f).

Time series of diatom Chla in different Longhurst provinces of the Atlantic are further extracted, in order to investigate whether the abrupt increase of diatoms during 2018-2019 took place in the whole Atlantic or only in some regions. Figure 4 presents large variability of the diatoms in different regions in terms of both magnitudes of Chla and temporal trends. In general, high latitudes and coastal regions, where diatom Chla is higher, present high inter-annual variation compared to the open ocean in lower latitudes. For instance, diatoms in the west coast of Africa (CNRY) are in general decreasing in the last two decades except a dramatic increase in late 2018 and spring 2019, following by a two-year decrease in 2020-2021. Despite of an obvious elevation in diatoms during 2018-2020, a significant decline of diatom in the last two decades is still found in the northwest coastal shelf region (NWCS), in consistency with the trend map shown in Fig. 3c. Slight increase is found in provinces in the gyres and equatorial region (NASW, NATR, WTRA, and SATL) with very low diatom Chla (mean Chla < 0.02 mg m^{-3}), and also in the Southern Ocean SSTC. The prominent increase observed during 2018-2019 is mostly contributed by the North Atlantic Ocean CNRY, NASE and NASW. Other provinces such as in the gyres with elevated diatom Chla since 2018, also contribute but only slightly to this increase due to much lower diatom Chla there compared to the other regions.

3.4 PFT phenology and anomaly of 2021

The status of the PFTs in the Atlantic Ocean is investigated specifically in 2021 to reflect the Atlantic ecological state and changes for this year as compared to the previous years. To understand better the yearly transition and shifting between different PFTs in the Atlantic Ocean, one of the phenology indicators, abundance maxima time, is mapped per-pixel for the

four PFTs (Fig. 5). Diatoms in the north Atlantic (> 35° N) reach the abundance maxima during late spring (April-May) but earlier (Jan-Feb) in the north Atlantic gyre. In the equatorial region the maxima months vary between May and August with the equator reaching the maxima the earliest (around May). In the southern hemisphere, diatoms reach maxima on average six months later than in the northern hemisphere, i.e., in the south Atlantic gyre July-August (austral winter) and October-December (late spring) in most of the Southern Ocean, which correspond well to the maxima seasons in the northern hemisphere. Haptophytes and dinoflagellates show similar patterns with diatoms, but on average bloom one month later than diatoms, indicating PFT dominance succession between diatoms and haptophytes in late spring and early summer. Prokaryotes over the whole Atlantic show a more complex and distinct seasonal cycle compared to the other three PFTs. The per-pixel phenology map presents that prokaryotes reach an abundance maximum from autumn to winter in latitudes > 20° N, and delay the maxima time with decreasing latitudes. In other regions the per-pixel maxima month normally spans a wider time window of three to five months, such as in the equatorial region from January to May, in the south Atlantic gyre from April to August, the western sector of the Southern Ocean January to April and the eastern sector November to January. Though geographically prokaryotes show more variation in the phenology, an overall inverse seasonal cycle is presented compared to diatoms, haptophytes and dinoflagellates, as depicted in Fig. 3a.

Anomalies in percentage of the four PFTs in 2021 compared to the average state of the last two decades are shown in Fig. 6. Diatom anomaly presents changes mainly in high latitudes, gyres and some coastal regions (such as CNRY). The anomaly shows mostly lower diatom Chla in high latitudes except for NWCS and the southeastern part of NADR where diatom Chla is increased. Opposed to that, diatom Chla of 2021 in the gyres is generally higher (~ 30%) compared to the 20-year average state. Note that changes are shown in percentage instead of the absolute values to enhance the visibility of small absolute changes, which in the gyres can be very sensitive, as diatom Chla is extremely low there (< 0.01 mg m^{-3}). Haptophyte anomaly presents changes in similar regions with diatoms but reversely in high latitudes, especially in the Southern Ocean, where a more prominent increase and also larger coverage are observed. Increase of haptophytes in the area north of the equator in WTRA is more significant than diatoms. Different from diatoms and haptophytes, prokaryotes reveal a very slight decrease in 2021 mostly in low latitudes within 20°N-20°S, with higher prokaryote Chla in the west coast of Africa especially CNRY, whereas only mild increase (< 20%) is found in high latitudes. Dinoflagellates show the most stable state in 2021 among the four PFTs with only a slight increase of Chla in the north Atlantic Ocean above 40°N and a small decrease in CNRY.

4. Discussion, conclusions and outlook

A systematic time series analysis of PFT in the Atlantic Ocean is carried out showing high potential of the Copernicus Marine Service satellite PFTs in monitoring the ecological state of the ocean at different scales. Due to different life spans and radiometric characteristics of satellite sensors, there are often inconsistencies and gaps between the same quantities retrieved from different sensors. Data continuity and quality assurance are therefore necessary to provide sound and continuous satellite observations enabling time series studies (Mélin and Franz, 2014; Sathyendranath et al., 2019). As preparatory work for such

a study aiming at long term monitoring of PFTs in the vast Atlantic Ocean, we applied a straightforward inter-mission bias correction as a preliminary trial using overlapped PFT products between the three sets of satellite data. Validation using in situ data shows no significant biases of PFTs derived from different sensors, indicating that the inter-mission offset was effectively corrected. Chla of different PFTs are more upscaled retrievals compared to bulk satellite OC products such as total chlorophyll a, coloured dissolved organic matter (CDOM) and absorption properties. Especially, it is still challenging to retrieve accurately prokaryotic phytoplankton because in the open ocean these are dominating in the low Chla areas for which the satellite signals are weaker. Therefore, higher uncertainties exist in these products (e.g., Brewin et al. 2017; Losa et al. 2017; Xi et al. 2021) as compared to uncertainties for other PFTs (see Table 2). In summary, our statistical results of PFT validation are comparable to the evaluations of satellite PFT products derived from different approaches, according to the Quality Information Documents (QUID) that have been published on CMEMS (Garnesson et al., 2022; Pardo et al., 2022). It is noteworthy that the bias correction targeted only on the Atlantic Ocean and might not be applicable to other ocean regions, which lead us to further explore a more generic method in the future for the global ocean. However, with these first investigations this study paves the way to promote satellite PFT products into long-term time series studies.

Satellite PFT products provide robust spatial distributions which are comparable to in situ data. The 20-year mean of the four PFTs has presented a trustable overview of how different PFTs vary and distribute spatially in the surface layer of the Atlantic Ocean. Diatoms, haptophytes and dinoflagellates share similar geographic patterns, showing higher abundance in high latitudes, coastal and equatorial upwelling regions where the nutrient level is generally high, and minimum abundance in the gyres especially for diatoms and dinoflagellates. Prokaryotes are more dominant in the gyres and low latitudes but contribute much less to the total biomass in high latitudes. Findings are consistent with previous studies of phytoplankton group and size classes (e.g., Hirata et al., 2011; Brewin et al., 2015; Losa et al., 2017) and are justified in detail in Xi et al. (2020). More recent studies by Bracher et al. (2020) and Brotas et al. (2022) based on in situ observations have also revealed similar PFT latitudinal distribution to our satellite observations. Furthermore, Brotas et al. (2022) point out that dinoflagellates can be underestimated in the pigment approach, due to their pigment variability; some species do not have the diagnostic pigment peridinin, and there are several heterotrophic species, where the pigments are absent or strongly reduced.

PFT time series of the last two decades are for the first time generated from multi-satellite observations. For the whole Atlantic Ocean, no significant trend was found for diatoms, haptophytes and dinoflagellates over the last 20 years, but a decline in prokaryotes was observed. However, the per-pixel trend maps revealed that regional trends are different from province to province, such as for diatoms, significant decrease was found in latitudes above 40° and west coast of Africa CNRY, similarly for haptophytes. There is a clear shift for prokaryotes in 2012: from 2003 to 2012, the average value is higher (0.064 mg m^{-3}), and the seasonality clearly defined, whereas from 2013 to 2020, seasonal variations are softened and the mean value is lower (0.053 mg m^{-3}). The retreat of MERIS in 2012 should not influence very much on the prokaryote data set for the following reasoning: firstly, such a decline was not found in other PFTs; secondly, MERIS observed more pixels in the coast and high latitude, we however focus on the open ocean and have excluded the coastal regions with bathymetry <200 m, and this study

covers the Atlantic Ocean between 50°N to 50°S. The main reason might be the relatively lower retrieval accuracy of prokaryotes compared to other PFTs as discussed above on the validation. Our previous work showed that all of the retrieval models for the three sets of sensor(s) have poorer performance for prokaryotic phytoplankton than for other PFT retrievals, this may cause weaker consistency of prokaryotes for the two decade period even after inter-mission correction. Nevertheless, coverage variability among different satellite missions should be taken into consideration in analyzing long-time series studies as the ability of the sensors to observe certain waters may differ (van Oostende et al. 2022). These findings in terms of 20-year trends still need to be evaluated further with both in situ measurements and numerical models, though available matchup data between in situ and satellite data are very sparse and disagreements between models and satellite observations also exist (Gregg & Rousseaux 2014). Indeed, a period of 20 years is considered not long enough for a robust trend analysis as the decadal variability might be too dominant, and for the Atlantic Ocean on average at least 35 years are needed to detect a climate driven trend in chlorophyll concentration as indicated in Hensen et al. (2010) and Hensen et al. (2016). Nonetheless, the 20-year long time series provides the opportunity to observe interesting patterns, such as the diatom increase during 2018-2019. Therefore, further investigation on biophysical interactions and linkage to climate is necessary to find evidence and interpret the findings extracted from PFT time series.

Phenology maps of the four PFTs correspond well with their mean annual cycles. Prokaryotes have distinct phenology compared to the other three PFTs which present similar annual cycles and close bloom maxima time on the general scale despite that haptophytes and dinoflagellates reach biomass maxima a bit later than diatoms in some regions. This section has chosen only one coarse phenological index, the time of the maxima, using monthly satellite products, which has shown the capability of the Copernicus Marine Service satellite PFTs in revealing PFT shifting and growth state in a larger scale than traditional means that rely on extensive ship-based measurements and long-term monitoring stations (e.g., Bracher et al., 2020; Nöthig et al., 2020; Yang et al., 2020). More other phenological indices, including the PFT growth duration, biomass amplitude, start and ending dates could be considered using higher temporal resolution products to fully understand the patterns and interannual variability of the PFT phenology (Soppa et al., 2016).

PFT anomaly of 2021 compared to the 20-year mean reveals mostly a slight decrease in diatoms above 40° N/S (except for the southeastern part of NADR) and a significant increase in haptophytes in most areas of the high latitudes, which corresponds well to the hypothesis of "Atlantification" proposing that smaller phytoplankton are expanding to the high latitudes (e.g., Nöthig et al., 2015; Neukermans et al., 2018; Oziel et al., 2020). Declining in silicate and nitrate concentrations might contribute to the decrease in diatoms in the north Atlantic as indicated in the Copernicus Ocean State Report 5 by von Schuckmann et al. (2021). In contrast to this, most changes in the Southern Ocean were found in latitudes higher than 40° S which is the region of the Great Calcite Belt. Deppeler and Davidson (2017) reviewed that climate induced changes such as higher temperature and shallow mixed layer depth are expected to alter the structure and function of phytoplankton communities in the Southern Ocean. Diatoms and haptophytes as two major groups there may be subject severely to these

changes. Interestingly, increase in haptophytes and decrease in diatoms indicated that the phytoplankton community structure is altering in the recent years which cannot be easily captured with observations other than satellite PFT time series.

In summary, this study illustrated the past and current PFT state in the Atlantic Ocean, and acted as the first step to promote long-term PFT observations serving as ocean monitoring indicators (OMI) implemented to the Copernicus Marine Service that enable time series analyses of PFT trends and inter-annual variability, to reveal potential climate induced changes in phytoplankton composition on multiple temporal and spatial scales.

Data availability

Data and products used in this study, as well as their availabilities and documentations are summarized in Table 1. In situ HPLC pigment and PFT data used for the validation of CMEMS PFT products are available on PANGAEA (https://doi.org/10.1594/PANGAEA.954738).

Author contribution

HX, AB, and AM conceptualized the study. HX designed and carried out the experiments. MB supported with the satellite products and SL helped with data analysis. VB, MG and IP supported substantially with the in situ data preparation. HX prepared the manuscript with contributions from all co-authors.

Competing interests

The authors declare that they have no conflict of interest.

Acknowledgments

We thank the European Union's Horizon 2020 Research and Innovation Programme under grant agreement 810139: Project Portugal Twinning for Innovation and Excellence in Marine Science and Earth Observation – PORTWIMS, ACRI-AWI joint project OLCI-PFT, Copernicus Marine – Innovation Service Evolution R&D Project (TIER2) "Global Long-term Observations of Phytoplankton Functional Types from Space (GLOPHYTS)" for funding. Copernicus Marine Service is implemented by Mercator Ocean International in the framework of a delegation agreement with the European Union. Astrid Bracher and Svetlana N. Losa were supported by DFG (German Research Foundation) Transregional Collaborative Research Center ArctiC Amplication: Climate Relevant Atmospheric and SurfaCe Processes, and Feedback Mechanisms (AC)3 (Project C03) and by the ESA S5P+Innovation Theme 7 Ocean Colour (S5POC) project (No 4000127533/19/I-NS). Svetlana N. Losa's work was also partly made in the framework of the state assignment of the Federal Agency for Scientific Organizations (FASO)

Russia (theme FMWE-2021-0014). We also thank Gavin Tilstone (PML), Giorgio Dall'Olmo (OGS) and Robert Brewin (University of Exeter) for AMT28 and AMT29 pigment data. Thanks to NASA, ESA and EUMETSAT for the SeaWiFS, MODIS, VIIRS, MERIS, and OLCI data, and specially the ACRI-ST GlobColour team for providing OLCI and merged ocean colour L3 products. Captain, crew, and expedition scientists are also acknowledged for their support at the expeditions. We finally thank Sorin Constantin and the other two anonymous reviewers who helped to improve this work by providing constructive comments.

References

Aiken, J., Pradhan, Y., Barlow, R., Lavender, S., Poulton, A., Holligan, P., & Hardman-Mountford, N. (2009). Phytoplankton pigments and functional types in the Atlantic Ocean: A decadal assessment, 1995-2005. Deep Sea Research Part II: Topical Studies in Oceanography, 56(15), 899–917. doi:10.1016/j.dsr2.2008.09.017

Amante, C., & Eakins, B.W. (2009). ETOPO1 1 arc-minute global relief model: Procedures, data sources and analysis (NOAA technical memorandum NESDIS NGDC-24). National Geophysical Data Center. Accessed in Febuary 2022.

Antoine, D., Morel, A., Gordon, H. R., Banzon, V. F. & Evans, R. H. (2005). Bridging ocean color observations of the 1980s and 2000s in search of long-term trends. J. Geophys. Res.: Oceans, 110, C06009.

Behrenfeld, M.J., O'Malley R.T., Boss, E.S., Westberry, T.K., Graff, J.R., Halsey, K.H., … & Brown, M. (2016). Revaluating ocean warming impacts on global phytoplankton. Nat. Clim. Change, 6, 3223–3330 (2016).

Bindoff, N.L., Cheung, W.W.L., Kairo, J.G., Arístegui, J., Guinder, V.A., Hallberg, R., … & Williamson, P. (2019). Changing Ocean, Marine Ecosystems, and Dependent Communities. In: IPCC Special Report on the Ocean and Cryosphere in a Changing Climate [H.-O. Pörtner, D.C. Roberts, V. Masson-Delmotte, P. Zhai, M. Tignor, E. Poloczanska, K. Mintenbeck, A. Alegría, M. Nicolai, A. Okem, J. Petzold, B. Rama, N.M. Weyer (eds.)]. Cambridge University Press, Cambridge, UK and New York, NY, USA, pp. 447–587. doi:10.1017/9781009157964.007

Bolaños, L. M., Karp-Boss, L., Choi, C. J., Worden, A. Z., Graff., J. R., Haëntjens, N., … & Glovannoni, S. J. (2020). Small phytoplankton dominate western North Atlantic biomass. The ISME Journal, 14, 1663–1674.

Bracher, A., Bouman, H.A., Brewin, R.J.W., Bricaud, A., Brotas, V., Ciotti, A.M., … & Wolanin, A. (2017). Obtaining phytoplankton diversity from ocean color: a scientific roadmap for future development. Front. Mar. Sci. 4, 1–15.

Bracher, A., Xi, H., Dinter, T., Mangin, A., Strass, V. H., von Appen, W.-J., & Wiegmann, S. (2020). High resolution water column phytoplankton composition across the Atlantic Ocean from ship-towed vertical undulating radiometry. Frontiers in Marine Science, 7, 235. doi:10.3389/fmars.2020.00235

Bracher, A., Brewin, R.J.W., Ciotti, A.M., Clementson, L.A., Hirata, T., Kostadinov, T., … & Organelli, E., (2022). Applications of satellite remote sensing technology to the analysis of phytoplankton community structure on large scales. In L.A. Clementson, R.S. Eriksen, & A. Willis (Eds.), Advances in Phytoplankton Ecology, pp. 217-244. Elsevier. doi: 10.1016/B978-0-12-822861-6.00015-7

Brewin, R.J.W., Sathyendranath, S., Jackson, T., Barlow, R., Brotas, V., Airs, R., & Lamont, T. (2015). Influence of light in the mixed-layer on the parameters of a three-component model of phytoplankton size class. Remote Sensing of Environment, 168, 437–450. doi:10.1016/j.rse.2015.07.004

Brewin, R. J. W., Tilstone, G. H., Jackson, T., Cain, T., Miller, P. I., Lange, P. K., et al. (2017). Modelling size-fractionated primary production in the Atlantic Ocean from remote sensing. Progress in Oceanography, 158, 130–149. doi:10.1016/j.pocean.2017.02.002

Brotas, V., Brewin, R.J.W., Sa, C., Brito, A.C., Silva, A., Mendes, C.R., … & Sathyendranath, S. (2013). Deriving phytoplankton size classes from satellite data: Validation along a trophic gradient in the eastern Atlantic Ocean, Remote Sensing of Environment, 134, 66-77. doi:10.1016/j.rse.2013.02.013

Brotas, V., Tarran, G.A., Veloso, V., Brewin, R.J.W., Woodward, E.M.S., Airs, R., … & Groom, S.B. (2022). Complementary Approaches to Assess Phytoplankton Groups and Size Classes on a Long Transect in the Atlantic Ocean. Front. Mar. Sci., 8, 682621. doi: 10.3389/fmars.2021.682621

Deppeler, S.L., & Davidson, A.T. (2017). Southern Ocean Phytoplankton in a Changing Climate. Front. Mar. Sci., 4, 40. doi:10.3389/fmars.2017.00040

Flanders Marine Institute (2009). Longhurst Provinces. Available online at https://www.marineregions.org/. Consulted on 21 March 2022.

Flombaum, P., Gallegos, J. L., Gordillo, R. A., Rincon, J., Zabala, L. L., Jiao, N., et al. (2013). Present and future global distributions of the marine Cyanobacteria Prochlorococcus and Synechococcus. Proceedings of the National Academy of Sciences of the United States of America, 110, 9824–9829. doi:10.1073/pnas.1307701110

Gregg, W. W. & Rousseaux, C. S. (2014). Decadal trends in global pelagic ocean chlorophyll: A new assessment integrating multiple satellites, in situ data, and models. J. Geophys. Res. Oceans, 119, 5921–5933.

Garnesson, P., & Bretagnon, M. (2022). QUID for OC TAC Products OCEANCOLOUR OBSERVATIONS GlobColour, Issue 2.0, Ref: CMEMS-OC-QUID-009-101to104-116-118, Date: 16 June 2022.

Gruber, N. (2011). Warming up, turning sour, losing breath: Ocean biogeochemistry under global change. Phil. Trans. R. Soc. A, 369, 1980-1996.

Gruber, N., Boyd, P.W., Frölicher T.L., & Vogt, M. (2021). Biogeochemical extremes and compound events in the ocean. Nature, 600, 395-407. doi:10.1038/s41586-021-03981-7

Head, E. J. H., & Pepin, P. (2010). Monitoring changes in phytoplankton abundance and composition in the Northwest Atlantic: a comparison of results obtained by continuous plankton recorder sampling and colour satellite imagery. Journal of Plankton Research, 32(12), 1649–1660. doi:10.1093/plankt/fbq120

Henson, S. A., Beaulieu, C., & Lampitt, R. (2016). Observing climate change trends in ocean biogeochemistry: when and where. Global change biology, 22(4), 1561-1571.

Henson, S. A., Sarmiento, J. L., Dunne, J. P., Bopp, L., Lima, I., Doney, S. C., … & Beaulieu, C. (2010). Detection of anthropogenic climate change in satellite records of ocean chlorophyll and productivity, Biogeosci. 7, 621–640.

Hirata, T., Hardman-Mountford, N. J., Brewin, R. J. W., Aiken, J., Barlow, R., Suzuki, K., … Yamanaka, Y. (2011). Synoptic relationships between surface Chlorophyll-a and diagnostic pigments specific to phytoplankton functional types. Biogeosciences, 8, 311–327. doi:10.5194/bg-8-311-2011

IOCCG. IOCCG Report 15: Phytoplankton Functional Types from Space (ed. Sathyendranath, S.) 156 pp. (International Ocean-Colour Coordinating Group, Dartmouth, Nova Scotia, 2014).

Käse, L., & Geuer, J.K. (2018). Phytoplankton Responses to Marine Climate Change – An Introduction, in S. Jungblut, V. Liebich, M. Bode (Eds.), YOUMARES 8 – Oceans Across Boundaries: Learning from each other, pp 55–71. Proceedings of the 2017 conference for YOUng MARine RESearchers in Kiel, Germany.

Kaufman, D.E., Friedrichs, M.A.M., Smith Jr., W.O., Hofmann, E.E., Dinniman, M.S., & Hemmings J.C.P. (2017). Climate change impacts on southern Ross Sea phytoplankton composition, productivity, and export, J. Geophys. Res. Oceans 122, 2339–2359.

Kulk, G., Platt, T., Dingle, J., Jackson, T., Jönsson, B.F., Bouman, H.A., … & Sathyendranath, S. (2020). Primary Production, an Index of Climate Change in the Ocean: Satellite-Based Estimates over Two Decades. Remote Sens., 12, 826. doi:10.3390/rs12050826

Lange, P.K., Werdell, P.J., Erickson, Z.K., Dall'Olmo, G., Brewin, R.J.W., Zubkov, M.V., … & Cetinić, I. (2020). Radiometric approach for the detection of picophytoplankton assemblages across oceanic fronts. Optics Express, 28(18), 25682–25705. doi:10.1364/OE.398127

Le Quéré, C., Harrison, S.P., Prentice, I.C., Buitenhuis, E.T., Aumont, O., Bopp, L., … & Wolf-Gladrow, D. (2005). Ecosystem dynamics based on plankton functional types for global ocean biogeochemistry models. Glob. Chang. Biol. 11, 2016–2040.

Longhurst, A. R. Ecological Geography of the Sea. 542pp., Academic Press, Burlington, MA, 2007. doi:10.1016/B978-0-12-455521-1.X5000-1

Losa, S.N., Soppa, M.A., Dinter, T., Wolanin, A., Brewin, R.J.W., Bricaud, A., … & Bracher, A. (2017). Synergistic Exploitation of Hyper- and Multi-Spectral Precursor Sentinel Measurements to Determine Phytoplankton Functional Types (SynSenPFT). Frontiers in Marine Science, 4, 1–22. doi:10.3389/fmars.2017.00203

Marinov, I., Doney, S.C., & Lima, I.D. (2010). Response of ocean phytoplankton community structure to climate change over the 21st century: partitioning the effect of nutrients, temperature and light. Biogeosci. 7, 3941–3959.

McClain, C.R. (2009). A decade of satellite ocean color observations. Ann. Rev. Mar. Sci. 1, 19–42.

Mélin, F., & Franz, B.A., (2014). Assessment of satellite ocean colour radiometry and derived geophysical products. In G. Zibordi, C. Donlon, & A. Parr (Eds.), Optical radiometry for oceans climate measurements, experimental methods in the physical sciences (Vol.47). Academic Press. doi:10.1016/B978-0-12-417011-7.00020-9

Moisan, T.A., Rufty, K.M., Moisan, J.R., & Linkswiler M.A. (2017). Satellite Observations of Phytoplankton Functional Type Spatial Distributions, Phenology, Diversity, and Ecotones. Front. Mar. Sci., 4, 189. doi:10.3389/fmars.2017.00189.,

Mouw, C.B., Hardman-Mountford, N.J., Alvain, S., Bracher, A., Brewin, R.J., Bricaud, A., … & Uitz, J. (2007). A consumer's guide to satellite remote sensing of multiple phytoplankton groups in the Global Ocean. Front. Mar. Sci., 4.

Neukermans, G., Oziel, L. & Babin, M. (2018). Increased intrusion of warming Atlantic water leads to rapid expansion of temperate phytoplankton in the Arctic. Glob. Chang. Biol. 24, 2545–2553.

Nöthig, E.M., Bracher, A., Engel, A., Metfies, K., Niehoff, B., Peeken, I., … & Wurst, M. (2015). Summertime plankton ecology in Fram Strait - a compilation of long-and short-term observations. Polar Res., 34, 23349.

Nöthig, E.M., Ramondenc, S., Haas, A., Hehemann, L., Walter, A., Bracher, A., … & Boetius, A. (2020). Summertime Chlorophyll a and Particulate Organic Carbon Standing Stocks in Surface Waters of the Fram Strait and the Arctic Ocean (1991–2015). Front. Mar. Sci., 7, 350. doi:10.3389/fmars.2020.00350

OC-CCI, 2020. Product User Guide for v5.0 Dataset. ESA Ocean Colour Climate Change Initiative –Phase 3.

Oziel, L., Baudena, A., Ardyna, M., Massicotte, P., Randelhoff, A., Sallée, J.-B., … & Babin, M. (2020). Faster Atlantic currents drive poleward expansion of temperate phytoplankton in the Arctic Ocean. Nature Comm., 11,1705.

Pardo, S., Jackson, T., Netting, J., Calton, B., & Howey, B. (2022). QUID for OC TAC Products Atlantic and Arctic Observation Products. Issue 2.0, Ref: CMEMS-OC-QUID-009-111 to114-121to124, Date: 16 June 2022.

Reyes-Prieto, A., Yoon, H. S., & Bhattacharya, D. (2009). Marine Algal Genomics and Evolution, in J.H. Steele (Eds.), Encyclopedia of Ocean Sciences (Second Edition) pp. 552-559, Academic Press. doi:10.1016/B978-012374473-9.00779-7

Sathyendranath, S., Brewin, R. J. W., Brockmann, C., Brotas, V., Calton, B., Chuprin, A., … & Platt, T. (2019). An ocean-colour time series for use in climate studies: The experience of the Ocean-Colour Climate Change Initiative (OC-CCI). Sensors, 19, 4285. doi:10.3390/s19194285

Soppa, M.A., Völker, C., & Bracher, A. (2016). Diatom Phenology in the Southern Ocean: Mean Patterns, Trends and the Role of Climate Oscillations. Remote Sensing, 8, 420. doi:10.3390/rs8050420

Uitz, J., Claustre, H., Morel, A., & Hooker, S.B. (2006). Vertical distribution of phytoplankton communities in open ocean: An assessment based on surface chlorophyll. Journal of Geophysical Research: Oceans, 111, C08005. doi:10.1029/2005JC003207

van Oostende, M., Hieronymi, M., Krasemann, H., Baschek, B., & Röttgers, R. (2022). Correction of inter-mission inconsistencies in merged ocean colour satellite data. Frontiers in Remote Sensing, 3, 1–17. doi:10.3389/frsen.2022.882418

Vidussi, F., Claustre, H., Manca, B.B., Luchetta, A., & Marty, J.-C. (2001). Phytoplankton pigment distribution in relation to upper thermocline circulation in the eastern Mediterranean Sea during winter. Journal of Geophysical Research: Oceans, 106(C9). doi:10.1029/1999JC000308

von Schuckmann, K., Le Traon, P., Smith, N., Pascual, N., Samuel Djavidnia, S., Gattuso, J., … & Zupa, W. (2021). Copernicus Marine Service Ocean State Report, Issue 5, Journal of Operational Oceanography, 14(sup1), 1-185. doi:10.1080/1755876X.2021.1946240

Xi, H., Losa, S. N., Mangin, A., Garnesson, P., Bretagnon, M., Demaria, J., … & Bracher, A. (2021). Global chlorophyll a concentrations of phytoplankton functional types with detailed uncertainty assessment using multi-sensor ocean color and sea surface temperature satellite products. Journal of Geophysical Research: Oceans, 126, e2020JC017127. doi:10.1029/2020JC017127

Xi, H., Losa, S.N., Mangin, A., Soppa, M.A., Garnesson, P., Demaria, J., … & Bracher, A. (2020). A global retrieval algorithm of phytoplankton functional types: Towards the applications to CMEMS GlobColour merged products and OLCI data. Remote Sensing of Environment, 240, 111704. doi:10.1016/j.rse.2020.111704

Xi, H., Peeken, I., Gomes, M., Brotas, V., Tilstone, G., Brewin, R.J.W., Dall'Olmo, G., Murawski, S., Wiegmann, S., Bracher, A. (2023). Phytoplankton pigment concentrations and phytoplankton groups measured on water samples collected from various expeditions in the Atlantic Ocean from 71°S to 84°N. PANGAEA. doi: 10.1594/PANGAEA.964738

Yang, B., Boss, E.S., Haëntjens, N., Long, M.C., Behrenfeld, M.J., Eveleth, R., & Doney, S.C. (2020). Phytoplankton phenology in the North Atlantic: Insights from profiling float measurements. Front. Mar. Sci., 7, 139. doi:10.3389/fmars.2020.00139

Tables

Table 1: Copernicus Marine Service products, own processed products, and in situ data used in this study.

Ref. No.	Product name & type	Documentation or data source
1	OCEANCOLOUR_GLO_BGC_L4_MY_009_104 Global Ocean – phytoplankton functional types derived from GlobColour SeaWiFS/MODIS/MERIS merged products for 2002-2011, from MODIS/VIIRS merged products for 2012-2016, and from Sentinel 3A OLCI for 2017-2021.	PUM: https://catalogue.marine.copernicus.eu/documents/PUM/CMEMS-OC-PUM.pdf QUID: https://catalogue.marine.copernicus.eu/documents/QUID/CMEMS-OC-QUID-009-101to104-116-118.pdf
2	Phytoplankton function types derived from SeaWiFS/MODIS/MERIS merged products for the period of January 2012 to April 2012	Reference: Xi et al. (2021)
3	Phytoplankton function types derived from Sentinel 3A OLCI product for the period of May 2016 to December 2016	Reference: Xi et al. (2021)
4	HPLC pigment based PFT data from various expeditions	Available on PANGAEA (Xi et al. 2023): https://doi.org/10.1594/PANGAEA.964738

Table 2: Statistical validation results of satellite derived PFT Chla (after inter-mission correction) as a function of in situ PFT Chla using least square fit in logarithmic scale. N: number of matchups; R^2: coefficient of determination; MDPD: median percent difference; RMSD: root-mean-square difference; definition equations of these terms were referred to Xi et al. 2020. Note that Slope, Intercept and R were calculated based on logarithmic scale. Median uncertainties calculated based on satellite per-pixel PFT uncertainty (equivalent to relative error in %, adapted from Xi et al. 2021) are also shown in the last column.

	N	Slope	Intercept	R^2	MDPD (%)	RMSD (mg m^{-3})	Median satellite PFT uncertainty (%)
Diatoms	192	0.71	-0.27	0.76	60.5	0.30	57.3
Haptophytes	191	0.95	-0.007	0.41	58.9	0.18	41.5
Prokaryotes	187	0.71	0.12	0.36	185	0.06	86.5
Dinoflagellates	144	1.07	0.04	0.66	59.1	0.07	74.3

Figures

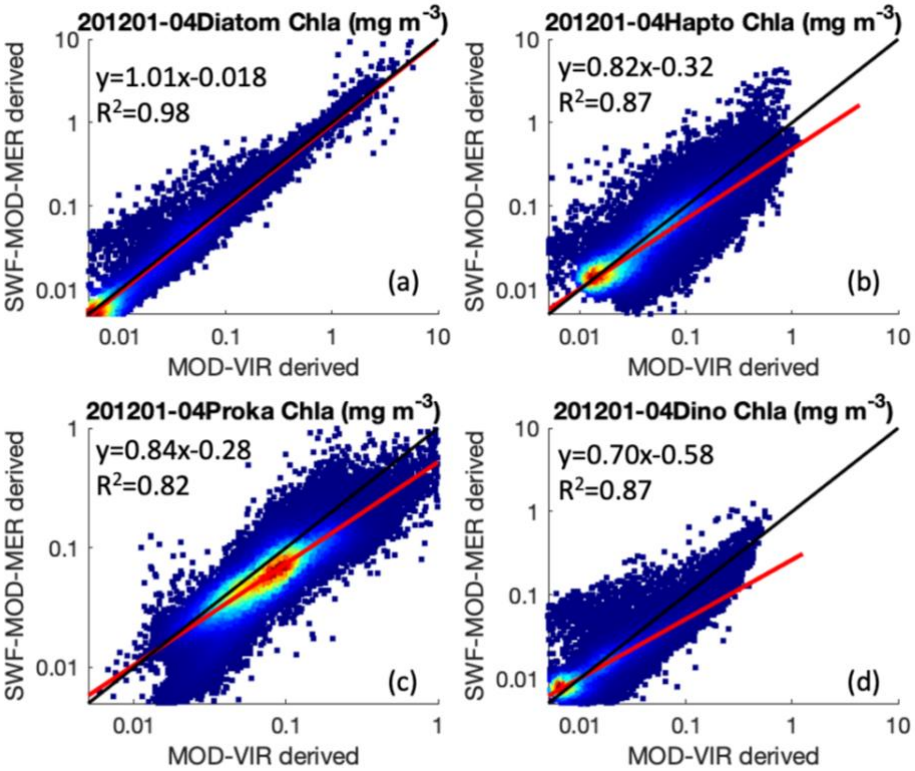

Figure 1: Scatterplots of monthly PFTs derived from SeaWiFS/MODIS/MERIS merged and MODIS/VIIRS merged Rrs data for the overlapping period January-April 2012. (a) diatoms, (b) haptophytes, (c) prokaryotes, and (d) dinoflagellates. The 1:1 line is shown in black and the linear regression line (using type II regression with per-pixel uncertainty) in red. R^2, slopes and offsets determined in log-10 scale are also presented.

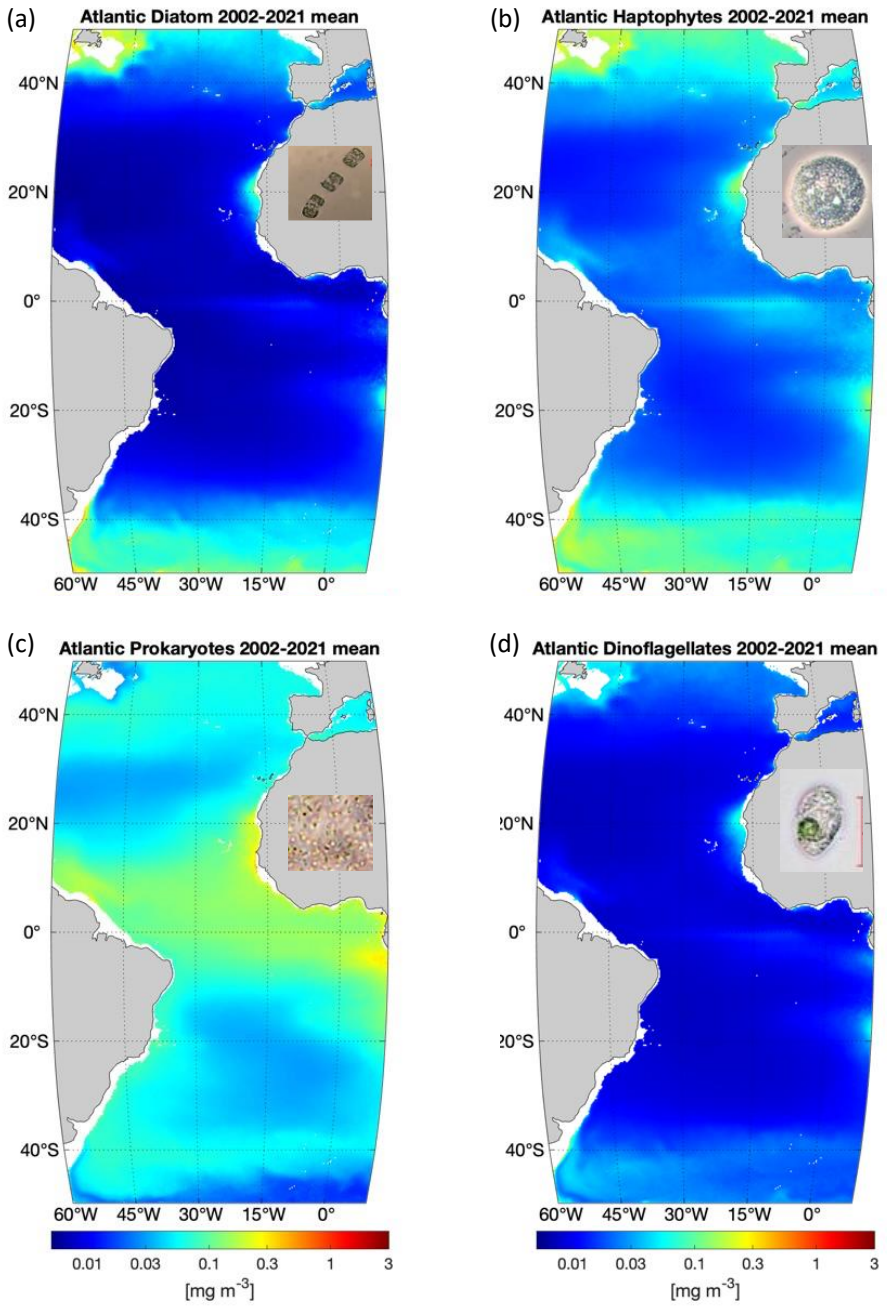

Figure 2: PFT climatology based on monthly PFT Chla products from 2002 to 2021: (a) diatoms, (b) haptophytes, (c) prokaryotes, and (d) dinoflagellates. Microscopic photos of the representative species for the four PFTs are presented (Photo credit: Alfred Wegener Institute).

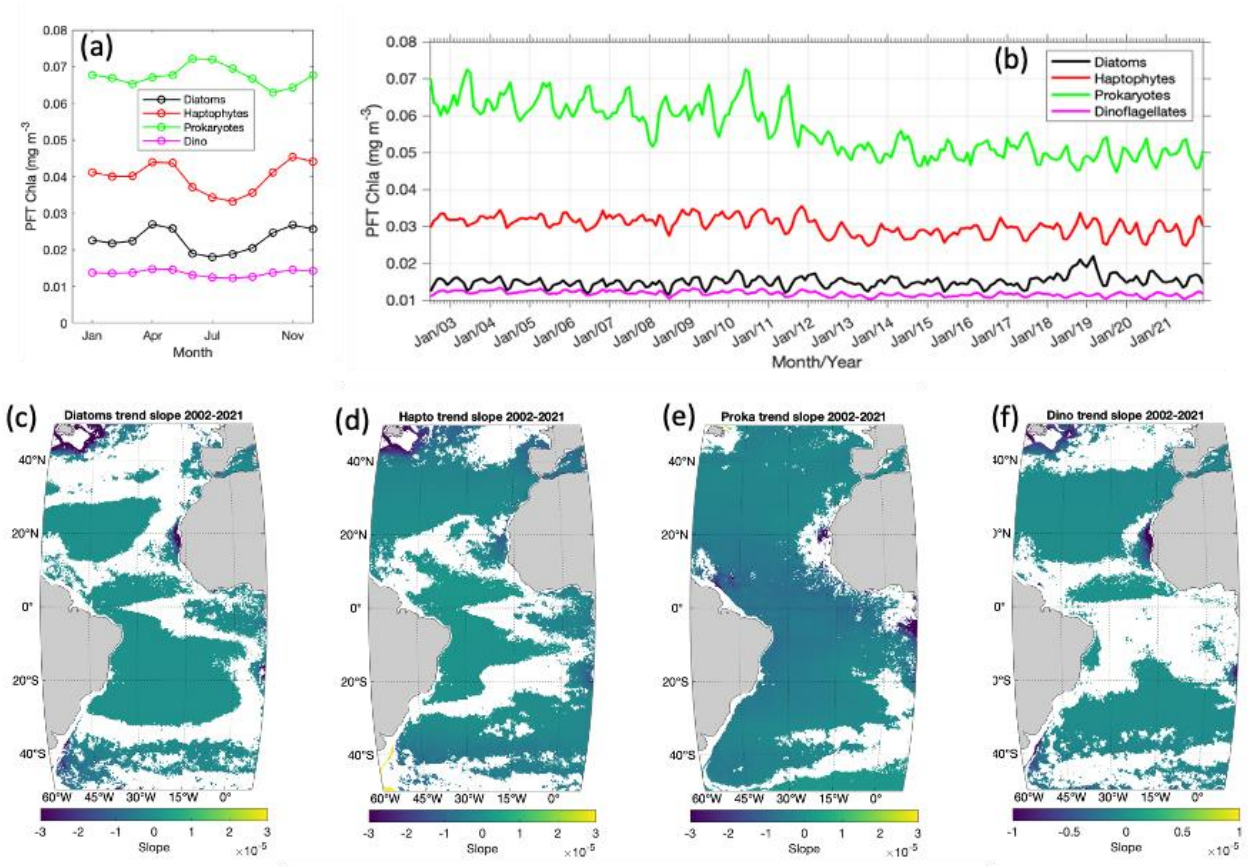

Figure 3: (a) Annual cycle of the four PFTs of diatoms, haptophytes, prokaryotes and dinoflagellates in the Atlantic Ocean (-50°S to 50°N, 60°W to 10°E), (b) 20-year time series from 2002 to 2021, and (c) per-pixel slope based on monthly Chla products of diatoms, (d) haptophytes, (e) prokaryotes and (f) dinoflagellates from 2002 to 2021 (where p<0.05 were shown, slope unit: Chla mg m^{-3} $month^{-1}$).

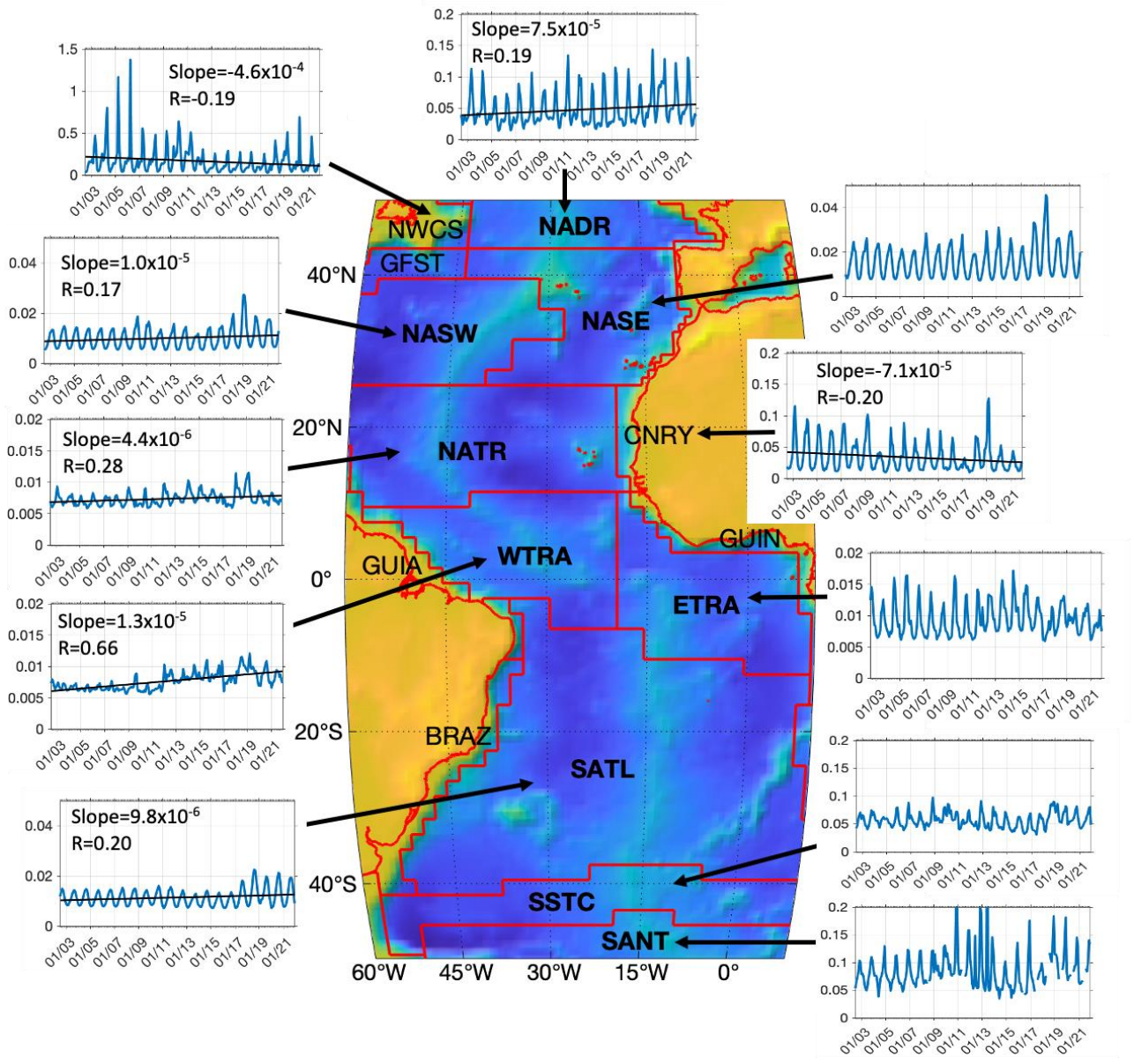

Figure 4: Time series of diatom Chla (unit: mg m^{-3}) in 11 Longhurst provinces in the Atlantic Ocean with bathymetric information based on ETOPO1 bathymetry (Amante & Eakins, 2009). Provinces according to Longhurst (2007) are: NADR for North Atlantic Drift Province, NWCS for Northwest Atlantic Shelves Province, NASW for North Atlantic Subtropical Gyral Province (West), NASE for North Atlantic Subtropical Gyral Province (East), NATR for North Atlantic Tropical Gyral Province, CNRY for Canary Current Coastal Province, WTRA for Western Tropical Atlantic Province, ETRA for Eastern Tropical Atlantic Province, SATL for South Atlantic Gyral Province, SSTC for South Subtropical Convergence Province, SANT for Subantarctic Water Ring Province, respectively. Trendlines with slopes (unit: Chla mg m^{-3} month^{-1}) and correlation coefficients are shown for provinces with significant trends ($p<0.05$).

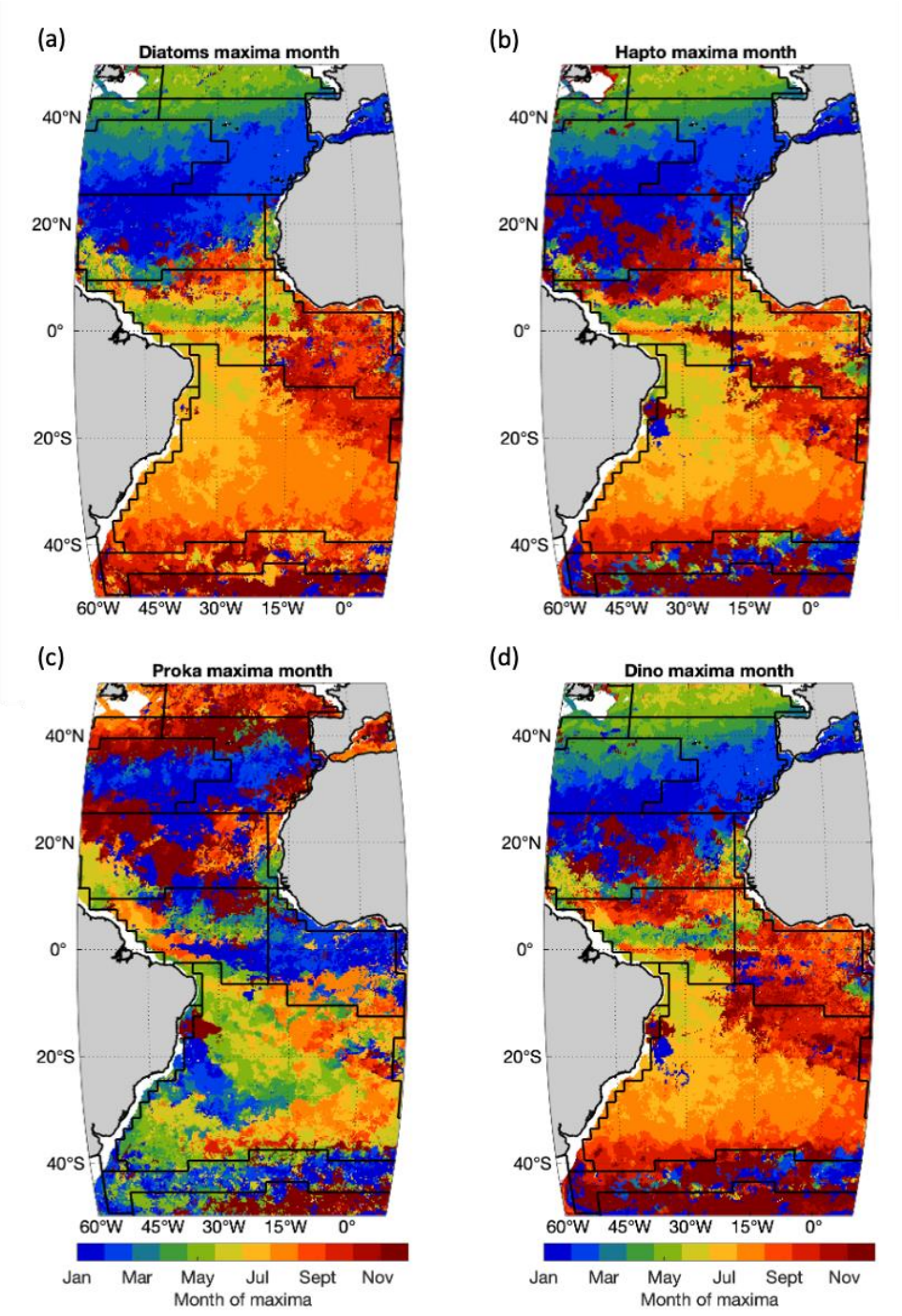

Figure 5: Occurrence month of PFT Chla maxima of 2021 in different provinces for (a) diatoms, (b) haptophytes, (c) prokaryotes and (d) dinoflagellates. Black lines indicate boundaries of Longhurst provinces as in Fig. 4.

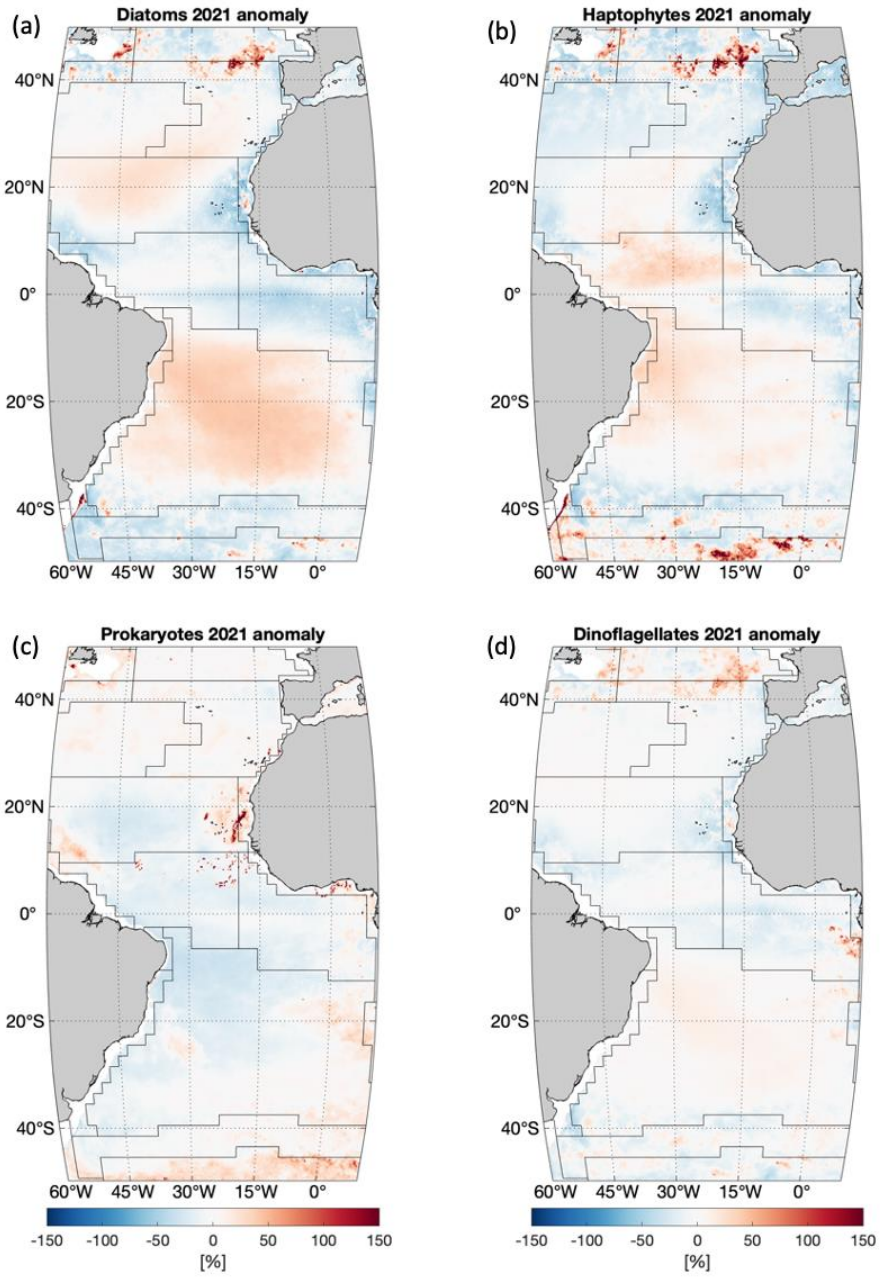

Figure 6: PFT anomaly in percentage [%] of 2021 compared to the 20-year mean for (a) diatoms, (b) haptophytes, (c) prokaryotes and (d) dinoflagellates. Anomaly in percentage is defined as (PFT_{2021} – climatology)/climatology*100. Black lines indicate boundaries of Longhurst provinces as in Fig. 4.